LA-UR- 09-01713

Approved for public release; distribution is unlimited.

Title: A repeating source of infrasound from the Wells, Nevada earthquake sequence

Author(s): Arrowsmith, Stephen, EES-17
Burlacu Relu, University of Utah
Whitaker, Rod, EES-17
Randall, George, EES-17

Intended for: Geophysical Research Letters

Los Alamos
NATIONAL LABORATORY
EST. 1943

A repeating source of infrasound from the Wells, Nevada earthquake sequence

Stephen J. Arrowsmith[1], Relu Burlacu[2], Rod Whitaker[1], George Randall[1]

(1) Los Alamos National Laboratory, P.O. Box 1663, Los Alamos, NM 87545

(2) University of Utah Seismograph Stations, University of Utah, Salt Lake City, UT 84112

Abstract

The Wells, Nevada earthquake of February 21, 2008, generated a complex seismo-acoustic wavefield. In addition to epicentral infrasound, the earthquake triggered a secondary source of infrasound, which was also initiated by subsequent aftershocks. By applying simple constraints on the propagation of seismic and infrasound waves, we show that the secondary source is an isolated peak that appears to efficiently generate infrasound through the interaction with seismic surface waves. By measuring peak-to-peak amplitudes of epicentral and secondary arrivals and correcting them for the effects of distance and winds, we find that epicentral arrivals fit with empirical relationships of Mutschlecner and Whitaker (2005) and Le Pichon et al. (2006), which form the basis for a proposed infrasound discriminant (Anderson et al., Pers. Comm.). In contrast, the secondary arrivals are much higher in amplitude, highlighting the importance of being able to separate epicentral and secondary arrivals for infrasonic event discrimination.

Introduction

Earthquakes can generate complex seismo-acoustic wavefields, consisting of pure seismic waves, pure acoustic waves, and waves that are generated by the interaction of the lithosphere and atmosphere. With regard to the latter type of wave, which is the focus of this paper, the interaction of seismic surface waves with the atmosphere is known to generate infrasound in regions that can be remote to the epicenter, due to the amplification of ground displacement by topography. Here, we refer to regions where infrasound is generated by such mechanisms as 'secondary sources', to distinguish them from infrasound generated at the earthquake epicenter. Previous studies of secondary sources from earthquakes have primarily been limited to single array observations of individual large events (Le Pichon et al., 2002, 2003, 2005). Le Pichon et al. (2006) attempt to reconstruct the secondary source regions for the magnitude 7.8 Chilean earthquake of June 13th, 2005 using three separate arrays. However, since secondary sources are thought to be largely directional (Le Pichon et al., 2003), and due to variations in propagation to each array, the authors reconstruct large distributed secondary source regions for each array separately.

In this study, we present the first detailed observation of a repeating secondary source from an earthquake and aftershock sequence. Our study extends previous studies in several ways: (1) the association is more robust (i.e., multiple observations of the same source provide statistical confidence in our interpretation); (2) we focus on understanding an isolated secondary source rather than a large distributed region, reducing the complexity of the problem; and (3) we are able to study variations in the source relative to the magnitude of the event.

As reported by the USGS, the Wells earthquake occurred at 14:16:02 UTC on February 21, 2008. The earthquake has a reported magnitude of 6.0, depth of 6.7 km, and epicenter located at (41.153°N, 114.867°W). As reported in a detailed seismological study of the event (ref Nevada paper), the earthquake moment tensor was consistent with a northeast striking normal fault dipping northwest or southeast. A sequence of aftershocks with similar depth and source mechanism followed the mainshock (ref Nevada paper).

In a previous study (Burlacu et al., 2009), we outlined the broad regional observations of infrasound from the Wells earthquake, which was recorded at five infrasound arrays located in Nevada, Utah, and Wyoming. Here, we focus on understanding a repeating signal at the BGU infrasound array in Utah, which we show below to be associated with a secondary source.

Observations

The mainshock and first three aftershocks of the Wells, Nevada earthquake sequence are detailed in Table 1 (reference Nevada paper). Figure 1 shows the observations of all four events at the BGU infrasound array. Only two of the events (Events 1 and 3) generated epicentral infrasound (i.e., infrasound generated at the epicenter and propagating through the atmosphere to the receiver as a pure acoustic wave). However, three events (Events 1, 2, and 3) generate a unique signal (shaded grey in Figure 1), which is observed at a backazimuth of 264° (16° off the great-circle backazimuth of 280°). The unique signals (Figure 2) are associated with identical phase velocities (0.37 km/s), and group velocities that range from 0.85 – 0.88 km/s (indicating a hybrid seismic to acoustic wave).

Interestingly, the amplitudes of these arrivals are larger than the corresponding epicentral infrasound signals (although much shorter in duration). Mutschlecner and Whitaker (2005) develop earthquake-scaling relations for wind-corrected amplitude, which have been utilized as an event discriminant since the corresponding amplitudes for explosions are greater (Anderson et al., Pers. Comm.). However, these studies utilize only epicentral infrasound. Clearly, our ability to separate epicentral infrasound from infrasound caused by secondary sources is critical for these discriminants to be useful.

Event Number	**Origin time**	**Magnitude**	**Epicentral infrasound**	**Secondary infrasound**
1 (Mainshock)	2008-02-21 14:16:02	6.0	Yes	Yes
2	2008-02-21 14:20:51	4.7	No	Yes
3	2008-02-21 14:34:43	5.1	Yes	Yes
4	2008-02-21 14:46:31	3.6	No	No

Table 1 – Summary of observations at BGU

Location

We can constrain the location of the secondary source by applying simple physical constraints on the seismic and infrasonic group velocities, and on the backazimuth. The constraints are as follows: (1) the seismic surface wave must propagate with a group velocity of between 3.0 and 3.5 km/s, (2) the infrasonic wave must propagate with a group velocity of between 0.28 and 0.35 km/s (this spans the full range of possible group velocities at this range), and (3) the deviation in backazimuth between the observed backazimuth and the actual backazimuth to the source must be less than 5° (accounting for measurement error and wind bias). Although the surface wave velocity could be better constrained using seismic data, it is far outweighed by the effect of uncertainty in the infrasound group velocity on the size of the location polygon. To locate the source we simply discretize a pie-shaped region with grid nodes (Figure 3), and for each grid node apply the constraint that $t_s+t_i=t_{obs}$. If this criterion can be satisfied for any grid node given the three constraints listed above, the grid node is a possible event location. The final location (including uncertainty) is a polygon that encloses all the possible locations.

As shown in Figure 4, the location polygon encloses a region that is mostly salt flats, but does include the edge of an isolated peak called Floating Island (reaching an elevation of 1000 ft above the surrounding salt flats). Given that there is a wide distributed region of salt flats near BGU, it seems unlikely that there is anything unique about this region of salt flat in terms of local site response. Thus, we conclude that the most plausible secondary source is Floating Island. This hypothesis would imply a wind bias of ~5°, and a relatively slow surface wave velocity.

The fidelity of models for infrasound propagation and associated specifications of relevant atmospheric parameters (temperature and winds) varies on a case-by-case basis. Recent studies have suggested that the combined use of state of the art 4D atmospheric specifications and simple ray-tracing algorithms may provide a statistical improvement for event location over simple bounding constraints. However, such a strategy cannot reliably predict observed phases for any given event. By modeling the propagation of infrasound using a 3D range-independent ray-tracing code (based on the Tau-P method of Garces et al., 1998) and state of the art G2S atmospheric specifications (Drob, 2004), we do not predict the observed arrivals from the Wells earthquake. Our results suggest that the secondary source is located in the 'zone of silence'; perhaps requiring a more sophisticated modeling strategy, beyond the scope of this paper. Here, we must rely upon simple bounding constraints on the location, such as those described above.

As discussed in Burlacu et al. (2009), the Wells earthquake was recorded at five infrasound arrays, including two additional arrays in Utah (EPU and NOQ) shown in Figure 4. Although secondary arrivals are observed at EPU (no clear secondary arrivals at NOQ), they do not correspond with this source location, implying that secondary sources associated with the Wells earthquake are dominated by local topography near the arrays.

Scaling Relationships

Mutschlecner and Whitaker (2005) developed scaling relationships for earthquake magnitude and duration (from ~ magnitude 4 – 7), which were corroborated for larger magnitudes by Le Pichon et al. (2006). They developed simple linear relationships for the duration and amplitude of epicentral infrasound. Here, we assess the fit for epicentral infrasound from the Wells earthquake, and contrast with observations from the secondary source.

Duration is difficult to measure for this event because the superposition of epicentral and secondary arrivals makes it hard to accurately measure the duration of epicentral infrasound at BGU. However, maximum peak-to-peak amplitudes are simpler to measure for epicentral and secondary arrivals since they are more robust to effect of superposition of arrivals. Normalized amplitudes (corrected for the effects of distance and stratospheric wind using Equation 1 from Mutschlecner and Whitaker, 2005) for both sets of arrivals are recorded in Table 2. Our findings show that, at BGU, secondary arrivals are much larger in amplitude than epicentral arrivals, although they are of noticeably shorter duration (Figure 1). Using the epicentral infrasound signals only, the corrected amplitudes (using Equation 1 from Mutschlecner and Whitaker, 2005) plot within the scatter of their observations.

Anderson et al. (Pers. Comm.) propose using the Mutschlecner and Whitaker (2005) relationships as the basis for an event discriminant, since observational studies suggest that the corresponding infrasonic amplitudes of underground explosions are greater at constant magnitude. However, as shown in Table 2, it is critical that epicentral arrivals can be separated from secondary arrivals, since incorrect identification could result in incorrect event identification. This is especially important in instances where the origin time is unknown, or where the source of secondary signals is close to the epicenter, since it would not be possible to identify secondary signals based on group velocity, as we have done in this paper.

Event Number	Epicentral log(μbar)	Secondary log(μbar)
1	0.4337	1.5897
2	N/A	-0.5586
3	-2.2146	-1.2143
4	N/A	N/A

Table 2 – Normalized amplitudes at BGU (corrected for the effects of distance and stratospheric wind using Equation 1 of Mutschlecner and Whitaker, 2005).

The issue of generation of infrasound from earthquakes remains poorly understood. Empirical observations by Mutschlecner and Whitaker (2005) and Le Pichon et al. (2006) have pointed towards a simple linear relationship between wind-corrected amplitude and earthquake magnitude for stratospheric returns. However, the generation of infrasound by secondary sources must be further understood for such a relationship to be of practical use as part of an infrasonic event discriminant. Furthermore, the effects of earthquake depth and source mechanism are not considered by Mutschlecner and Whitaker (2005) or Le Pichon et al. (2006). These effects could provide significant scatter in such scaling relations. Aftershock sequences could provide an invaluable mechanism for improving our understanding of these issues since, as is the case of the sequence of four events considered in this paper (ref Nevada paper), the depths and source mechanisms are very similar, allowing us to isolate the effect of earthquake magnitude.

Conclusions

Previous studies of secondary infrasound from earthquakes have found broad correlations between topographic highs and source generating regions for major – great earthquakes. Our observations and analyses extend such studies in 3 primary ways: (1) we focus on much smaller events (M<6.0), (2) we observe a repeating source, providing robust association, (3) our observations highlight an isolated source, rather than a broad-scale region. Our findings highlight the importance of improving our understanding of the physical generation of infrasound from secondary sources, since our ability to discriminate between earthquakes and explosions infrasonically hinges on our ability to separate epicentral and secondary infrasound. We show that aftershock sequences provide a unique opportunity to improve our understanding of earthquake-generated infrasound, by allowing us to separate effects of earthquake magnitude, depth, and source mechanism on infrasonic amplitudes. Finally, our work suggests that duration may be an unreliable discriminant since it is highly sensitive to the superposition of epicentral and secondary arrivals. Further work is required to investigate these issues in more detail, using an extensive dataset of robust associations of earthquake-generated infrasound.

References

Burlacu, R., Arrowsmith, S., Hayward, C., and Stump, B., Infrasonic Observations from the February 21, 2008 Wells Earthquake, Submitted to the Wells Earthquake Volume, USGS, 2009.

Drob, D., Atmospheric Specifications for Infrasound Calculations, InfraMatics, 5, 6-13, 2004.

Garces, M., Hansen, R.A., and Lindquist, K.G., Traveltimes for infrasonic waves propagating in a stratified atmosphere, Geophys. J. Int., 135, 255-263.

Le Pichon, A., Guilbert, J., Vega, A., Garces, M., and Brachet, N., Ground-coupled air waves and diffracted infrasound from the Arequipa earthquake of June 23, 2001, Geophys. Res. Lett., 29, doi:10.1029/2002GL015052.

Le Pichon, A., Guilbert, J., Vallee, M., Dessa, J. X., and Ulziibat, M., Infrasonic imaging of the Kunlun Mountains for the great 2001 China earthquake, Geophys. Res. Lett., 30, doi:10.1029/2003GL017581, 2003.

Le Pichon, A., Herry, P., Mialle, P., Vergoz, J., Brachet, N., Garces, M., Drob, D., and Ceranna, L., Infrasound associated with 2004-2005 large Sumatra earthquakes and tsunami, Geophys. Res. Lett., 32, doi:10.1029/2005GL023893, 2005.

Le Pichon, A., Mialle, P., Guilbert, J., and Vergoz, J., Multistation infrasonic observations of the Chilean earthquake of 2005 June 13, Geophys. J. Int., 167, 838-844.

Mutschlecner, J.P., and Whitaker, R.W., Infrasound from earthquakes, J. Geophys. Res., 110, doi:10.1029/2004JD005067.

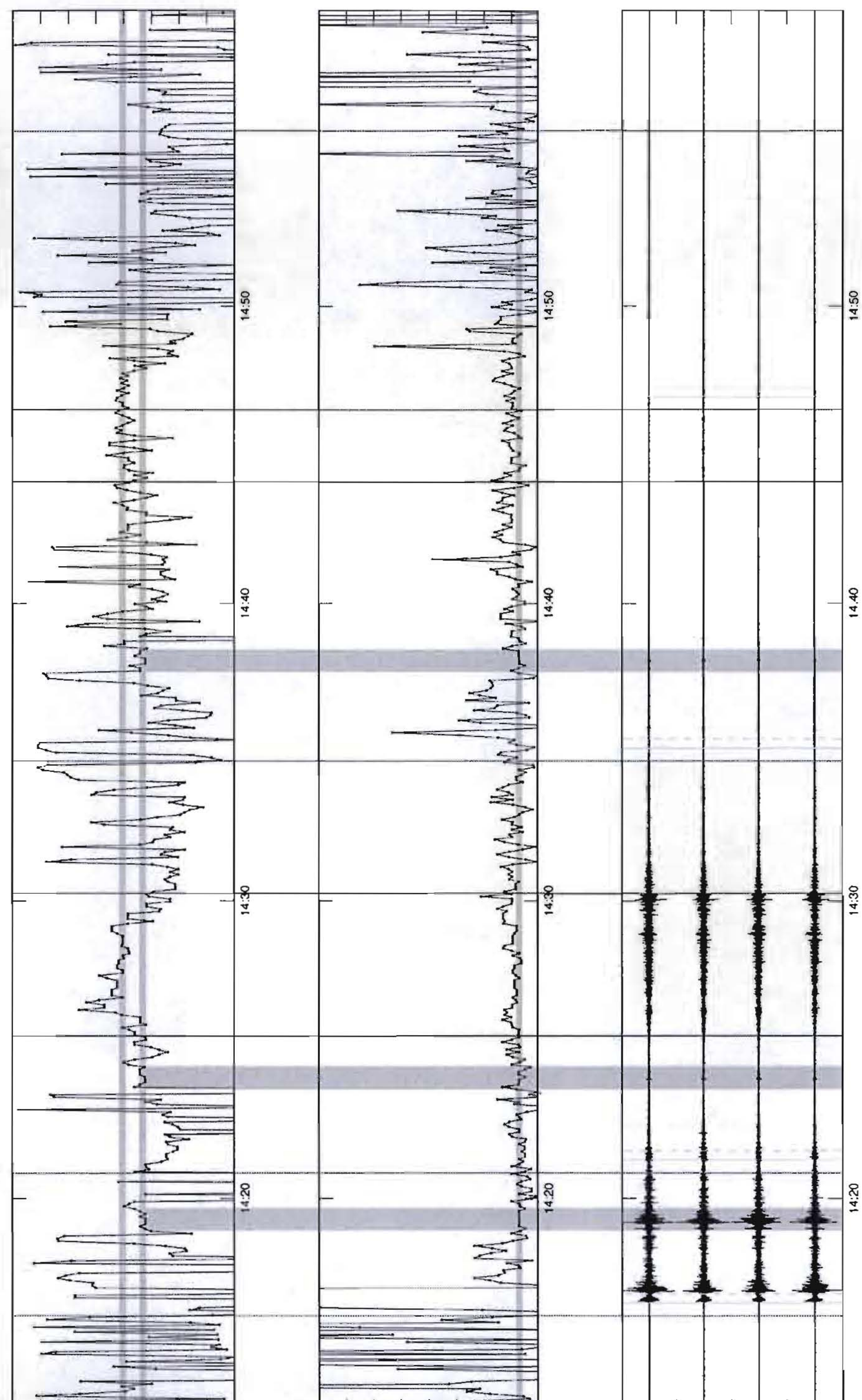

Figure 1 – Acoustic observations at BGU. Bottom panel: Acoustic traces at each array element, bandpass filtered from 1 – 5 Hz. Red lines denote the origin times of Events 1 – 4 (Table 1), green lines denote corresponding predicted arrival times for seismic waves (Pg – solid, Lg – dashed), blue lines denote predicted arrival times for epicentral infrasound. Center and top panels represent phase velocity and backazimuth respectively, obtained using InfraMonitor (ref). Vertical grey shaded regions highlight arrivals from the secondary source.

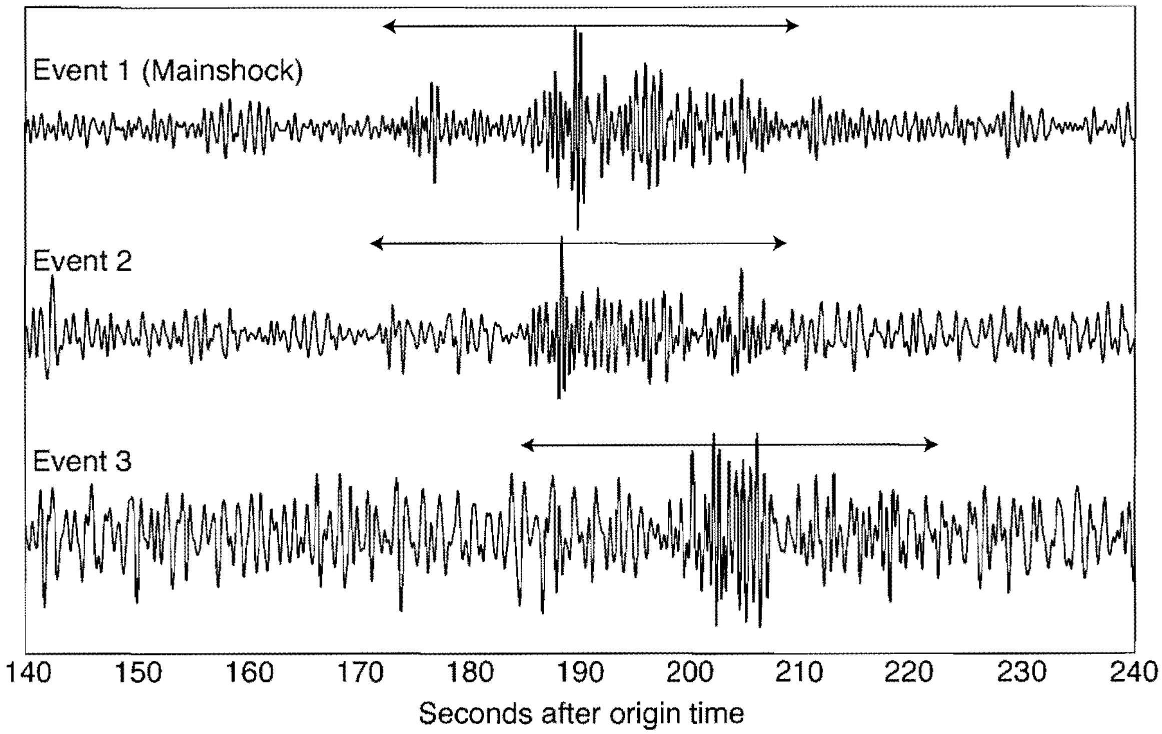

Figure 2 – Blow-up of the observations of signals from the secondary source for Events 1 – 3 (Table 1). Each signal is associated with a similar group velocity (i.e., arrival times of major energy packets are similar with respect to each event origin time) and frequency content.

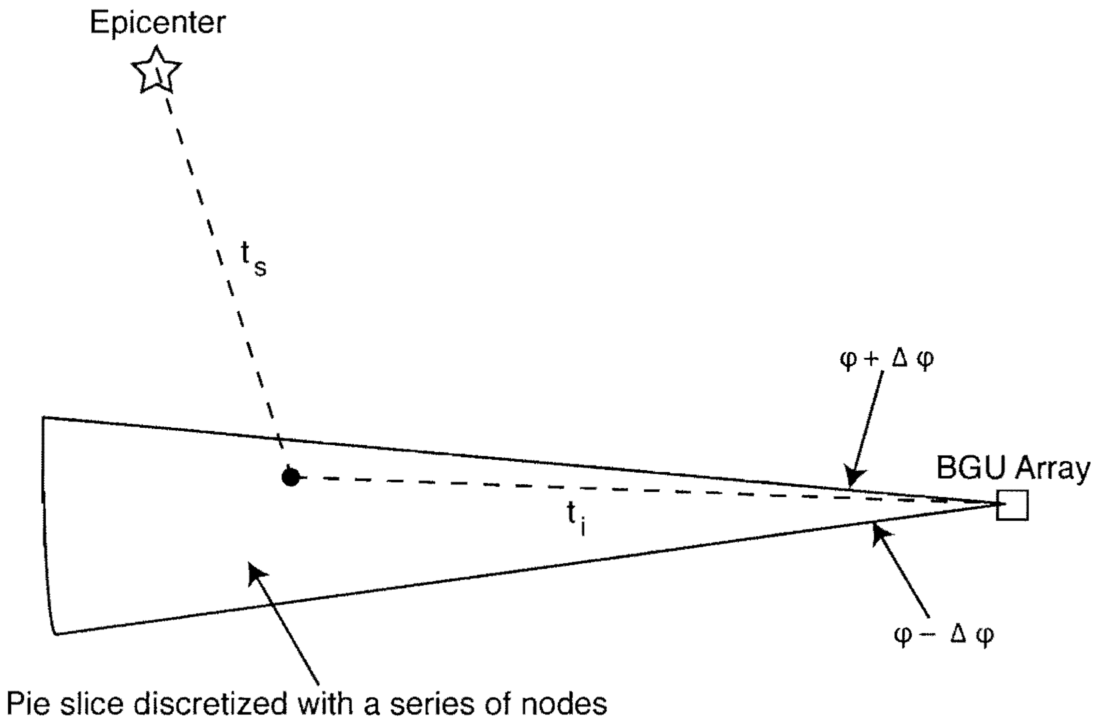

Figure 3 – Schematic diagram illustrating the method used to locate the secondary source.

Figure 4 – Map showing location of secondary sources recorded at BGU